C. M. Hood, R. C. Schroter, D. J. Doorly, E. J. S. M. Blenke and N. S. Tolley
J Appl Physiol 107:1195-1203, 2009. First published Jul 16, 2009; doi:10.1152/japplphysiol.91615.2008

J Appl Physiol 107: 1195–1203, 2009.
First published July 16, 2009; doi:10.1152/japplphysiol.91615.2008.

Computational modeling of flow and gas exchange in models of the human maxillary sinus

C. M. Hood,[1] R. C. Schroter,[1] D. J. Doorly,[2] E. J. S. M. Blenke,[2,3] and N. S. Tolley[3]

Departments of [1]Bioengineering, [2]Aeronautics, and [3]Otolaryngology, St. Mary's Hospital, Imperial College London, London, United Kingdom

Submitted 18 December 2008; accepted in final form 10 July 2009

Hood CM, Schroter RC, Doorly DJ, Blenke EJ, Tolley NS. Computational modeling of flow and gas exchange in models of the human maxillary sinus. *J Appl Physiol* 107: 1195–1203, 2009. First published July 16, 2009; doi:10.1152/japplphysiol.91615.2008.—The present study uses numerical modeling to increase the understanding of sinus gas exchange, which is thought to be a factor in sinus disease. Order-of-magnitude estimates and computational fluid dynamics simulations were used to investigate convective and diffusive transport between the nose and the sinus in a range of simplified geometries. The interaction between mucociliary transport and gas exchange was modeled and found to be negligible. Diffusion was the dominant transport mechanism for small ostia and large concentration differences between the sinus and the nose, whereas convection was important for larger ostia or smaller concentration differences. The presence of one or more accessory ostia can increase the sinus ventilation rate by several orders of magnitude, because it allows a net flow through the sinus. Estimates of nitric oxide (NO) transport through the ostium based on measured sinus and nasal NO concentrations suggest that the sinuses cannot supply all the NO in nasally exhaled air.

nose; airflow; computational fluid dynamics; nitric oxide

THE MAXILLARY SINUSES, the largest of the human paranasal sinuses, are particularly susceptible to infection, as excess fluid cannot easily drain from them by gravity (32). The resulting sinusitis is a painful and often chronic condition that affects ~15% of the population of the United Kingdom (17) and has significant economic implications, due to medical costs and lost productivity, making it the ninth most expensive condition for employers in the United States in 1999 (10). Despite its prevalence and importance, the causes of sinusitis are not well understood, but it is thought that the condition involves impaired mucociliary transport and reduced sinus ventilation (27). Surgical interventions for sinusitis often aim to increase the ventilation of the sinuses, but the quantitative effects of changing sinus geometry on sinus ventilation are not fully known.

The maxillary sinuses are located behind the cheeks and are joined to the middle meatus of the nasal cavity by the maxillary ostium (32). The ostia often lie at an angle to the coronal plane of a single computed tomography (CT) slice; a schematic depiction of the nose, sinuses, and ostia adapted from a CT image is shown in Fig. 1. The detailed anatomy of the nose and sinuses is complex and highly variable between individuals, but several studies have assessed typical dimensions and configurations. The consensus is that the maxillary sinuses are typically 10–15 ml in volume, with a 3- to 6-mm-diameter, 6-mm-long ostium. The proportion of sinuses with one or more extra or accessory ostia is highly controversial, with rates of 2–44% found in different studies; rates were generally higher in cadaver studies and lower in in vivo studies. Most accessory ostia are found in the fontanelles, a region of the nasal wall where there are only mucosal membranes, no bony component; this region is particularly susceptible to damage (32). More accessory ostia have been found in studies of sinus and ostium anatomy using cadaver heads (25, 26, 34, 37), as moist nasal mucosal tissue can shrink after death because of drying and the fixing processes. The fontanelle membranes may also have been damaged during drying and investigation. In contrast, in vivo studies (15) may have found fewer accessory ostia if they were covered with a thin film of mucus or were in an inaccessible location.

The causal link between the presence of accessory ostia and sinus disease is unclear; it has been suggested that sinus infections can damage the fontanelles to create accessory ostia (18) and also that accessory ostia may be a cause of sinus disease by disturbing mucociliary transport or allowing easier pathogen access to the sinuses (23). One possible disease scenario is that an initial acute nasal or sinus infection damages the fontanelles, creating an accessory ostium, which leads to recurrent sinus infections.

In vivo measurements of sinus ventilation are rare because of the small size and inaccessibility of the cavities. In his classic work in 1932, Proetz (29) reported measurements of the variation of pressure in the nose and sinuses during breathing. He calculated that this variation of pressure and, thus, volume (as described by Boyle's law) would cause a small movement of air into and out of the sinuses, equivalent to a quarter of the volume of a typical ostium, such that ≥1 h would be required to replace the whole volume of air in a sinus. Later, Drettner (8) and Rantanen (30) reported that the pressure in a sinus with an open ostium follows the variation in the nose very closely. This result means that the pressure changes in the nose during the breathing cycle do not drive flow into or out of the sinus, except by the associated volume change, contrary to speculation by Törnberg et al. (35). Proetz was not able to measure the pressure gradient along the nose, which is much smaller than the pressure changes during the breathing cycle. His resulting assumption of a uniform pressure throughout the nose led him to reason that accessory ostia could not increase the exchange rate of sinus air (28).

In an early attempt to measure the time to wash a gas out of the maxillary sinuses, Aust and Drettner replaced the air in model (3) and real (2) sinuses with pure nitrogen, then electronically tracked the concentration of oxygen in the sinus as air reentered. Later studies using two isotopes of xenon, radio-

Address for reprint requests and other correspondence: C. M. Hood, Dept. of Bioengineering, Imperial College London, South Kensington Campus, Royal School of Mines Bldg., London SW7 2AZ, UK (e-mail: c.hood06@imperial.ac.uk).

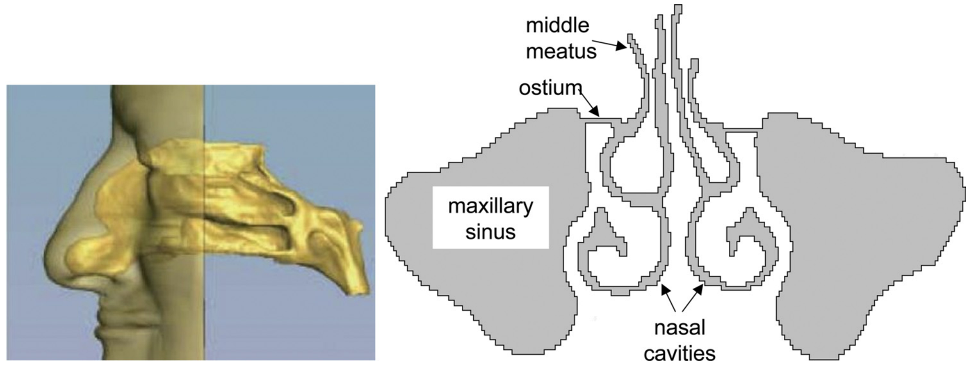

Fig. 1. Anatomy of nose and sinuses: reconstruction from computed tomography (CT) image (*A*) and schematic representation based on CT slice (*B*).

active ^{133}Xe (4, 40) and radiodense ^{129}Xe (16, 22) gases, concur with the finding of Aust and Drettner that the typical time for washout of a healthy sinus, assumed to have a single ostium, is 5–10 min, whereas washout times for diseased sinuses tend to be much longer. The results of these studies may be skewed by the difficulties of introducing into sinuses a sufficient concentration of gas to produce clear images, particularly if the sinus has rapid exchange, and also by the artificially high concentration differences between the nose and the sinus. As with most other published results related to sinuses, sinus ventilation times show extremely wide inter- and intra-individual variations.

It has been demonstrated that nasal air contains a higher nitric oxide (NO) concentration than air from the lower or oral airways, whereas the maxillary sinuses maintain a significantly higher NO concentration than the nasal cavity (19). In addition, sinus mucosa has been found to contain significantly more of one type of NO synthase (NOS) than nasal mucosa (19), but healthy nasal mucosa was found to contain mainly the other two forms of NOS (13). The absolute and relative NO production rates per unit area of mucosa in the nose and sinuses have not been reported, but a few values for total NO production by the nose and/or the sinus have been reported (9).

It has been suggested that the NO generated within the nasal sinuses is transported into nasal air via the ostia, thus providing the majority of the NO gas detected in nasal sampling. However, the extent to which sinus NO can contribute to observed nasal NO levels is not clear. In this study, the possible rates of this NO transport are estimated and the associated sinus production rates are predicted and compared with estimated and measured production levels.

Recently, several studies have found increased NO concentration in air exhaled from the nose during humming (11, 21, 24, 38), suggesting that sound at vocal frequencies increases NO transport out of the sinuses. Earlier work also highlighted an increase in aerosol deposition in the sinuses when the aerosol was excited by acoustic waves (12, 20, 31). Both of these findings indicate that acoustic phenomena can be very important for sinus transport, but the underlying physical processes have not been investigated.

The present study aims to increase the understanding of sinus ventilation by modeling the putative physical processes involved. Simple order-of-magnitude estimates and detailed computational modeling have been used to explore the relative importance of the different mechanisms. Simplified geometries were used to represent the shape of the sinus cavity, to enable straightforward manipulation of geometry, and to separate the effects of different anatomic variations.

METHODS

The sinus is characterized (Fig. 2) as a large truncated cone, joined to a rectangular channel representing the middle meatus of the nasal cavity by a small tube representing the ostium, with dimensions taken from anatomic studies in the literature. Most of the geometry variations considered affect the ostium, because this is thought to control the magnitude of transport between the sinus and the nose. The model geometries discussed in this study are summarized in Table 1. All the geometries have sharp corners between the sinus and ostium and the nasal cavity and ostium, but this is not thought to affect the flow significantly.

Model B was chosen as the standard single-ostium geometry for comparisons and additional modeling, and *model H* was chosen as the standard double-ostium geometry. The separation between ostium centerlines on the models with an accessory ostium was 10 mm along the *y*-axis, parallel to the middle meatal flow.

Order-of-Magnitude Calculations

Simple first-order and one-dimensional (1-D) calculations were performed based on Boyle's law, Fick's law, and similar relations to estimate transport rates. These initial estimates were used for comparison with computational and experimental results and allow a swift assessment of the significance of different factors in sinus ventilation.

A simple estimate for the time taken for the air in the sinus to be replaced by diffusion was obtained using Fick's law of first-order

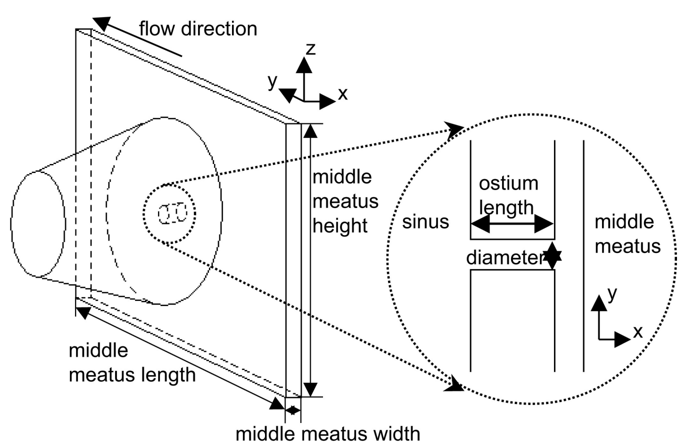

Fig. 2. Simplified single-ostium geometry. Middle meatus flow is in the positive *y*-direction. Typical middle meatus dimensions are 70 mm long × 3 mm wide × 50 mm high.

Table 1. *Summary of model geometries*

	Ostium 1		Ostium 2	
Model	Φ	λ	Φ	λ
A	2	6		
B	3	6		
C	3	3		
D	4	6		
E	6	6		
F	6,3	6		
G	3,6	6		
H	3	6	3	6
I	3	6	3	6
J	4.5	6	4.5	6
K	6	6	6	6
L	3	6	6	6
M	6	6	3	6

Φ, Diameter; λ, length (all in mm). *Models F* and *G* have elliptical ostia. *Model I* has double the normal pressure difference along the middle meatus. *Model L* has a 3-mm ostium upstream and a 6-mm ostium downstream; *Model M* has a 6-mm ostium upstream and a 3-mm ostium downstream.

diffusion. The computed estimate was intended to be a comparison with the experimental study carried out by Aust and Drettner (3) described above. The experimental oxygen concentration follows an approximately exponential approach to atmospheric conditions, which suggests that a 1-D and first-order diffusion model may be sufficient to describe this situation.

The rate of change of the quantity of oxygen in the sinus is set equal to the diffusive flux through the ostium, such that

$$\mathrm{V}d[O_2]_S/dt = DA([O_2]_N - [O_2]_S)/L$$

and

$$[O_2]_S = (1 - \exp(-DAt/\mathrm{V}L))[O_2]_N$$

where V is the sinus volume, $[O_2]_S$ and $[O_2]_N$ represent oxygen concentrations in the sinus and the nose, respectively, expressed as volume fractions, *D* is the diffusion coefficient of oxygen in nitrogen, *A* is the cross-sectional area of the ostium, and *L* is the length of the ostium. If we assume that $[O_2]_N$ is constant in time and solve for the time (T_{90}) taken for $[O_2]_S$ to reach 0.9 $[O_2]_N$ from an initial value of 0, $T_{90} = -\mathrm{V}L/DA \ln(0.1)$.

Estimation of NO transport

Order-of-magnitude estimates were also made for NO transport on the basis of Fick's law for diffusion and the computational dluid dynamics (CFD) convective transport values. The range of NO concentrations measured and reported in the nose and maxillary sinus is very wide, so the values from two studies (1, 19) were used to examine the expected range of transport.

If all the air inhaled with no initial NO content is brought to the nasal NO concentration, then NO must be added to it at a rate

$$[NO]_N{*}\mathrm{V}_B/T$$

where $[NO]_N$ is the nasal concentration (assumed constant), V_B is the volume of a breath (tidal volume), and *T* is the duration of the inspiration. NO can be transported through the ostium convectively, at a rate of $\dot{Q}[NO]_S$, where $\dot{Q}$ is the volumetric flow rate (from CFD), and diffusively at a rate of $DA([NO]_S - [NO]_N)/L$ (from Fick's law). The sinus mucosa must produce NO equal to the quantity transported through the ostium to maintain a constant internal concentration. The range of sinus production rates reported in previous studies (9) was used for comparison with the calculated transport values.

CFD Studies

Using the stylized geometric shapes for the sinus and associated ostium (see above), we first defined the sinus interior using a meshing technique. The commercial CFD software Fluent 6.3.26 was then used within this structure to model fluid flow alone and in conjunction with diffusive transport. Fluent's companion program Gambit 2.3.16 was used for mesh generation, and Tecplot 360 was used for solution visualization. Quadrilateral meshes were created for two-dimensional (2-D) models, and hexahedral meshes were used for three-dimensional (3-D) models. 2-D models are less computationally expensive than 3-D models, so higher mesh densities were used. Varying mesh sizes were used to capture the flow details efficiently; the smallest cells were used in and close to the ostium, whereas larger cells were allowed in distant regions of the middle meatus. The convergence of the solution with increasing mesh density is given in the APPENDIX. It was not possible to model <2-mm-diameter ostia in 3-D because of limited computational resources. Convection simulations solved only the Navier-Stokes equations for fluid dynamics, whereas later simulations also solved transport equations for an inert species. All convection-only simulations were performed in 2-D and 3-D, whereas simulations involving diffusion were quantitatively meaningful only in 3-D.

Boundary conditions and assumptions. Pressure boundary conditions taken from a previously published CFD simulation of a whole, anatomic nose model (7) were applied to each end of the middle meatus section of the present model; the peak air velocity in the meatus matched the value from the nose model. The flow conditions were quiet breathing, where the pressure difference along the middle meatus was 2 Pa and the peak meatus velocity was 1.2 m/s. The geometry was assumed to be rigid because of the bony nature of the nasal walls. The walls were modeled with a no-slip condition and assumed to be stationary, except for a few cases modeling mucociliary transport.

RESULTS

Convection

Standard single-ostium model (model B). The CFD prediction of the steady flow in the middle meatus and sinus shows channel flow through the middle meatus, which provides a shear driving force at the nasal cavity end of the ostium. This shear from the middle meatus produces vortices in the ostium, as expected from the classic fluid dynamics problem of a driven cavity (14, 33), and is shown in Fig. 3. The velocity magnitudes in the ostium decrease rapidly from the middle meatus toward the sinus, from $O(10^{-2})$ to $O(10^{-5})$ m/s. The ostium vortices extend slightly into the sinus, but there is no net flow into or out of the sinus. Vortical flow is also set up in the sinus, with velocities on the order of 10^{-5}–10^{-7} m/s. The numerical integration of positive or negative velocities across the ostium-sinus interface allows the fluxes into and out of the sinus to be calculated and, thus, an estimate to be made for the time required to replace the sinus air, if the sinus is assumed to be a well-mixed vessel. For the standard-geometry ostium, the time required to replace 90% of sinus air by convection would be 84 h. This time is likely to be a lower-bound estimate, as exchange between the ostial and sinus vortices may be limited.

Geometry variations: diameter and length. In the standard ostium geometry (3 mm diameter, 6 mm long), there are two vortices in the ostium. Increasing the ostium diameter, or reducing its length, has the effect of removing the second vortex, as predicted by the driven cavity solution. This qualitative change of flow pattern increases the velocity magnitudes and reverses the orientation of flow at the ostium-sinus interface. For example, the standard geometry has peak velocities across the

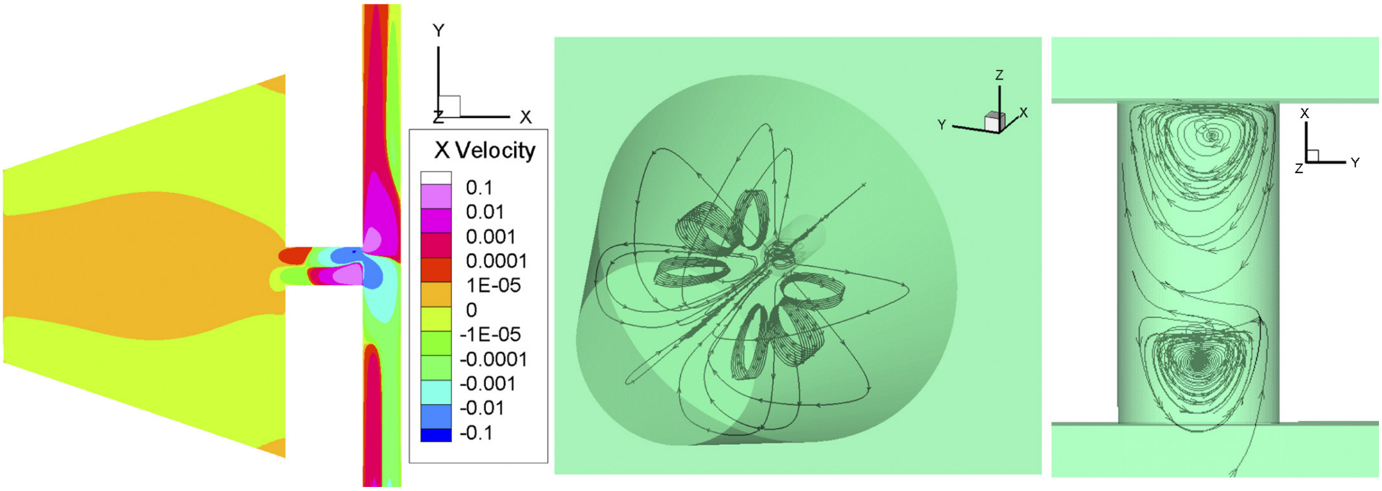

Fig. 3. *x*-Velocity contours: sinus and ostium streamlines for *model B*.

interface of $\pm 2.5 \times 10^{-5}$ m/s; reducing the length to 3 mm (*model C*) increases the peak interface velocities to $\pm 4 \times 10^{-3}$ m/s, and increasing the diameter to 6 mm (*model E*) increases the peak interface velocities to $\pm 2 \times 10^{-2}$ m/s. The corresponding estimated exchange times decrease to 83.4 and 5.2 min, respectively. The increased interface velocities resulting from a single vortex in the ostium will also increase the velocities within the sinus, promoting gas mixing and exchange.

Elliptical ostia. Real ostia tend to be elliptical, rather than circular, in cross section, so two models (*models F* and *G*) were created with elliptical ostia to investigate its effect. In each case, the ostium had a cross-sectional 6-mm long axis, 3-mm short axis, and 6-mm transverse length. In *model F*, the long axis of the ostium cross section was parallel to the flow direction in the middle meatus; in *model G*, it was perpendicular to the flow. Ostium streamlines for *models F* and *G* are shown in Fig. 4.

In *model F*, the flow pattern in the ostium was similar to that in a cylindrical ostium of the same length and diameter (both 6 mm), except it was more symmetrical in the *y*-direction. The peak transverse velocity magnitudes at the ostium-sinus interface were, however, considerably smaller, $\pm 3 \times 10^{-3}$ m/s as opposed to $\pm 2 \times 10^{-2}$ m/s.

Model G, by contrast, showed a flow pattern different from that of the "equivalent" cylindrical ostium with the same diameter parallel to the flow (3 mm diameter, 6 mm long). The first horizontal vortex near the middle meatus in the cylindrical ostium is present, but the second vortex near the sinus has a strong vertical component that is not found in the cylindrical ostium solution. There is also more asymmetry in the *y*-direction in the elliptical than in the cylindrical ostium flow solution. The peak velocities across the ostium-sinus interface are $\pm 1 \times 10^{-4}$ m/s, which are larger than in the equivalent cylindrical ostium.

Other variations. Models with curved or tilted ostia, ostia positioned off-center in the sinus, alternative sinus shapes, or a curved or tapered middle meatus were created, and the flow was assessed. These geometry variations had some influence on the detailed flow patterns but very little effect on the velocity magnitudes and ventilation calculations.

Auxiliary ostia. With the same boundary conditions at each end of the middle meatus as for the single-ostium model, the standard double-ostium geometry (*model H*) has a pressure difference between the ostia of ~0.1 Pa. The pressure difference generates a flow into the sinus through the upstream

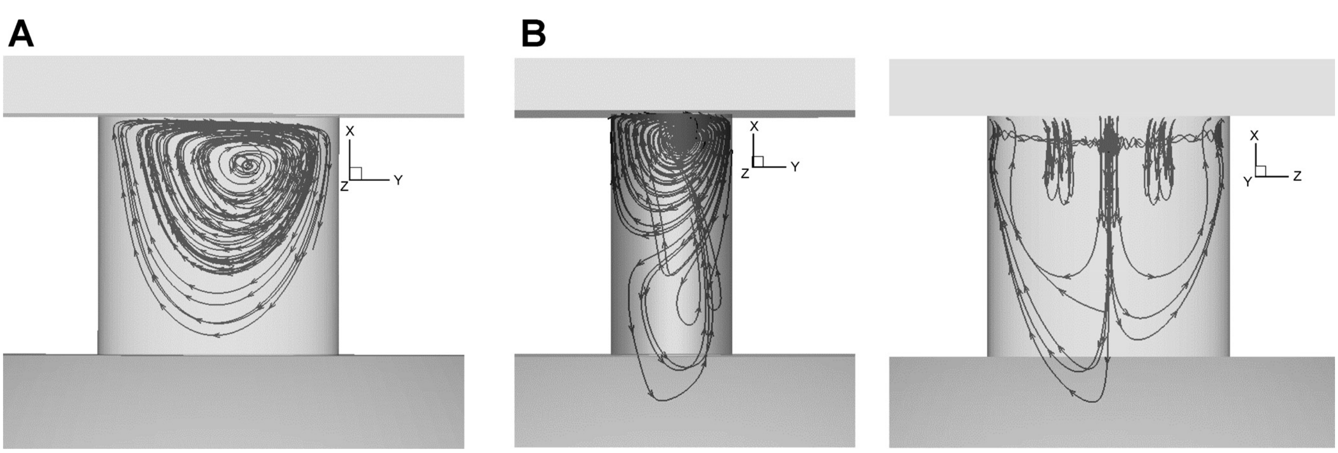

Fig. 4. Ostium streamlines for *model F* (*A*; long-axis parallel to middle meatus flow) and *model G* (*B*; short-axis parallel to middle meatus flow).

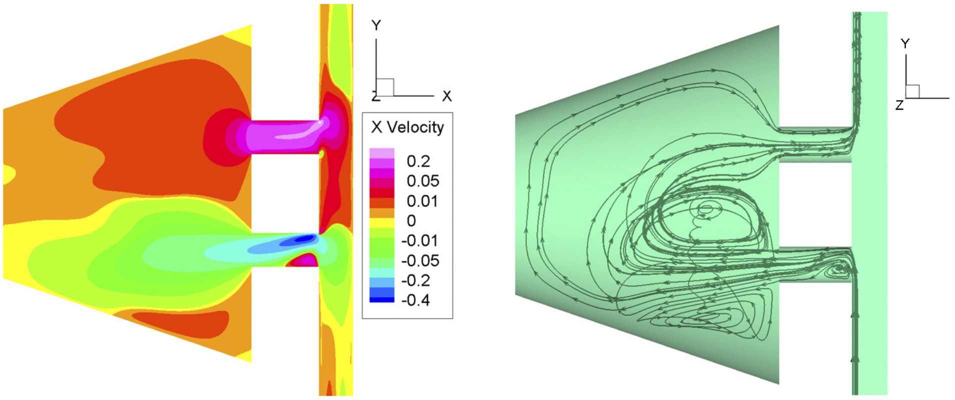

Fig. 5. *x*-Velocity contours and sinus streamlines for *model H.*

ostium and a flow out of the sinus through the downstream ostium of 7.2 × 10^{-7} m^3/s (Fig. 5).

The air in a 10-ml sinus would be completely replaced by this flow after ~14 s, if we assume sustained unidirectional flow conditions in the middle meatus and plug flow through the sinus. Alternatively, if it is assumed that the sinus behaves as a well-mixed vessel (6) because the streamlines cover the whole volume (Fig. 5), it is predicted that 90% of the air in the sinus will be exchanged in 31.9 s. A summary of the flow rates and estimated sinus gas exchange times for the different accessory ostium geometries is given in Table 2.

Model I was run with twice the normal pressure drop along the middle meatus to explore the effect of increased breathing flow rate, which led to an increase in the pressure difference between the ostia to 0.3 Pa. The resulting flow through the sinus was 9.4 × 10^{-7} m^3/s, leading to an estimated 90% exchange time of 24.5 s.

Mucociliary Transport Effects

The potential effects on the sinus flow characteristics of the moving mucous layer on the walls of the sinus, ostium, and nasal cavity can be modeled by assigning appropriate velocities to the walls of the Fluent simulation. Proetz (28) provided a diagram of observed mucociliary transport patterns in the sinuses. We used a range of mucociliary transport values (1–10 mm/min) based on values in the literature for nasal and tracheal transport, as no measures of sinus mucociliary transport velocity were available. The modeling was initially performed in 2-D and later in 3-D, with extension programs written and added to Fluent to set the 3-D wall velocities on the surfaces of the sinus.

The inclusion of a mucous wall movement changes the gas flow pattern in the sinus by increasing the proportion of flow close to the walls and the velocity magnitudes (Fig. 6) but does not significantly increase the gas velocities in the ostium. Therefore, it was not found to reduce the gas exchange time of the sinus, either alone or in conjunction with diffusion.

Table 2. *Summary of double ostium ventilation time estimates*

Model	Ostium 1 Φ	Ostium 1 λ	Ostium 2 Φ	Ostium 2 λ	Q̇, $m^3 \cdot s^{-1}$	T_{90}, s
H	3	6	3	6	7.2×10^{-7}	31.9
J	4.5	6	4.5	6	1.7×10^{-6}	13.5
K	6	6	6	6	2.6×10^{-6}	8.9
L	3	6	6	6	1.1×10^{-6}	20.9
M	6	6	3	6	1.1×10^{-6}	20.9

Q̇, volumetric flow rate; T_{90}, time to replace 90% of sinus air.

Diffusion

The convection simulations described above were used as the basis for simulations of diffusive transport. The unsteady, nonreacting transport of oxygen and nitrogen was added to the existing steady solutions for velocity and pressure. The initial conditions of the unsteady simulation were that the oxygen concentration was zero in the sinus and ostium and atmospheric in the nasal cavity. The upstream boundary condition (inhaled air) was also at atmospheric concentration. The average oxygen concentration in the sinus was written out at every time step, and the time for the concentration to reach 90% of atmospheric was noted.

A 1-D estimate using Fick's law and a 6-mm-diameter ostium gave a 90% exchange time of 3.4 min, which is considerably longer than 2.5 min in a physical model reported by Aust and Drettner (3). 3-D CFD models with diffusion alone and combined convection and diffusion matched these results closely, showing that convection is responsible for the increase in transport found by Aust and Drettner compared with pure diffusion (Fick's law). A summary of results for other ostium diameters and modeling combinations is given in Table 3. Convective transport had an insignificant effect on the 2- and 3-mm-diameter ostia but did increase ventilation for 4- and 6-mm diameter ostia, as can be seen in the variation of sinus oxygen concentration with time (Fig. 7).

Some 2-D convection-diffusion simulations were run with reduced flow rate through the middle meatus, which increased the time taken for sinus exchange. This slowing of exchange is thought to be due to the reduced convective transport being insufficient to maintain the atmospheric concentration at the middle meatus end of the ostium, thus reducing the concentration gradient along the ostium and slowing diffusion into the sinus.

NO Transport Estimates

The calculations described in METHODS give a range of NO transport rates required to supply all measured nasal NO as 4 × 10^{-9}–3 × 10^{-8} mol/s (5,000–50,000 nl/min). However, convection through a standard ostium and diffusion between the

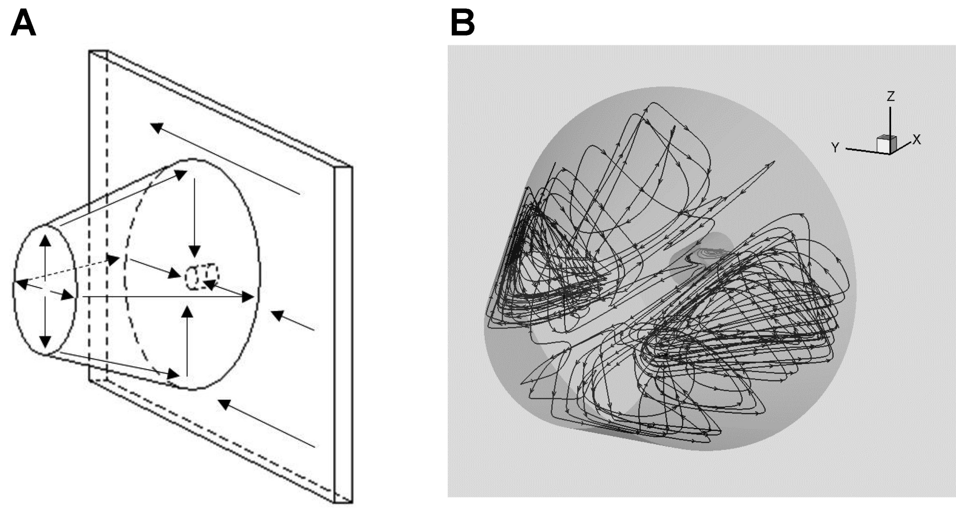

Fig. 6. *A*: modeled mucociliary transport velocity directions. *B*: sinus streamlines from model simulating effects of mucociliary transport.

measured sinus and nasal concentrations can only provide NO at 2×10^{-12}–4×10^{-11} mol/s, equivalent to 3–60 nl/min. Measured rates of NO production by sinus mucosa are 217–455 nl/min (1×10^{-10}–3×10^{-10} mol/s) (9), which is an order of magnitude smaller than the nasal NO flow rate but an order of magnitude larger than that required to maintain a constant concentration in the sinus.

Alternatively, it is possible to consider the rate of NO production per unit area of mucosa, if it is assumed that production is uniform across the mucosal surfaces. The nasal mucosal surface area is $\sim 10 \times 10^{-3}$ m^2, so if this produced all the measured NO, the rate per unit area would be 3×10^{-7}–3×10^{-6} mol·m^{-2}·s^{-1}. The sinus mucosa has a surface area of 24×10^{-6}–50×10^{-6} m^2, so a production rate of 7×10^{-5}–1×10^{-3} mol·m^{-2}·s^{-1} would be required to supply all the nasal NO. In contrast, if the sinus produces only enough NO to compensate for the convective and diffusive losses calculated above, the required NO production rates per unit area of mucosa are 4×10^{-8}–1×10^{-6} mol·m^{-2}·s^{-1}, similar to the estimated nasal production rate.

DISCUSSION

Limitations of Sinus Ventilation

The results of this study suggest that the natural ventilation rate of a sinus with a single ostium is extremely slow. Indeed, such limited ventilation may be protective for the sinus, as it would help prevent drying of its mucosal surface and maintain a near-sterile environment with high NO concentrations and minimal pathogen access.

Table 3. *Summary of single ostium sinus exchange times*

	T_{90}, min				
			CFD		
Φ, mm	Aust and Drettner (3)	Fick's law	Conv	Diff	Conv + Diff
2	18.5	30.5	1×10^7		
3		13.6	5,040	12	12
4	4.2	7.6	840	7.1	6.4
6	2.5	3.4	5.2	3.4	2.3

All ostia are 6 mm long. Fick, estimate from Fick's law (1st-order diffusion); CFD, computational fluid dynamics; Conv, convection; Diff, diffusion.

Steady flow in the middle meatus cannot produce net flow through a single ostium, as this would violate the conservation of mass. The shear flow in the meatus does, however, cause motion in the ostium and sinus, which enhances diffusive transport. Wider or shorter ostia have much faster velocities and, therefore, are capable of higher transport rates; for example, the 6-mm-diameter ostium (*model E*) has an estimated convective exchange time of 5.2 min compared with 5,040 min for the 3-mm-diameter ostium (*model B*).

The size, orientation, and velocity magnitudes of the vortices in the ostium are the same in the 2-D and 3-D models for all the geometries presented. The geometry and flow conditions for a single ostium are equivalent to a tube with a small side branch when there is no net flow in the branch, as investigated in analytic work by Tutty (36). Streamlines in the ostium for the 2-D and 3-D models (Fig. 8) show a close match with independent analytic results and the present approach of numerical modeling compared with the analytic work of Tutty (Fig. 15 in Ref. 36). The streamlines and vortex patterns also match well the analytic predictions of driven cavity flow patterns (14, 33), which are often used as a test case for CFD systems.

The models with elliptical ostia highlight the complexity of the interaction between 3-D nasal geometry and flow. The difference between their flow and implied gas exchange rates, despite their identical cross-sectional areas, and the differences between their flow and that of circular ostia of the same diameter in the direction of flow show that the size, shape, and orientation of the ostium relative to the nasal flow can contribute to the flow magnitude and ventilation rate in a sinus.

Differences of Double-Ostium Sinuses

The models with an accessory ostium show considerably increased transport rates in a double-ostium sinus with ostia exposed to even very slightly different pressures compared with a single-ostium sinus. The different pressures could be caused by two ostia having different axial locations or being exposed to different flow conditions in the nose. The increased

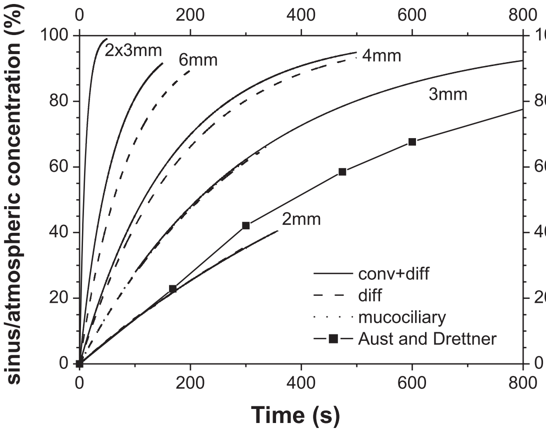

Fig. 7. Time course of sinus oxygen concentration with data from computational fluid dynamics simulations and Aust and Drettner (3). conv, Convection; diff, diffusion. Dimensions are ostium diameter; all ostia are 6 mm long.

ventilation of a double-ostium sinus is due to a qualitative difference in the flow: the single-ostium sinus can be considered a reservoir of fluid attached to the nose, whereas the double-ostium sinus offers an alternative flow path in parallel with the nose. Thus only a sinus with two or more ostia can have a net flow through it.

The findings of this study contradict Proetz's conclusion that an accessory ostium cannot increase the ventilation of a sinus (28), which has been widely quoted out of its original context. From the computer modeling and theoretical considerations, it is clear that an accessory ostium can significantly increase sinus ventilation. It is possible, however, that such an increased level of ventilation is not functionally beneficial. Possible adverse effects include *1*) reduced NO concentration, if the rate of convective transport through the ostia exceeds the rate of production, leading to impaired mucociliary function, and *2*) increased pathogen entry into the sinus. Mucosal drying is another potential problem in sinuses with increased ventilation, as sinus mucosa has a lower density of mucus-producing glands and serous cells than the main nasal cavity (27). The closer the upstream ostium is to the nostril, the greater the risk of mucosal drying, as the air entering the sinus will be less well conditioned. Accessory ostia can also lead to circular mucociliary transport, which can introduce pathogens from other parts of the nasal cavity into the sinus (23).

The flow through the sinus can be increased by increasing the spacing of the ostia to increase the driving pressure difference across the sinus, with the assumption that the pressure gradient along the middle meatus is unchanged. If the pressure gradient along the middle meatus is increased, as implemented in *model I*, the flow through the sinus will also be increased. However, the increase in sinus flow is not proportional to the increase in pressure difference between the ostia, because the resistance of the ostia-sinus path is higher than the parallel middle meatus path; consequently, the middle meatus will carry a larger proportion of the overall flow increase. Increasing the diameter of the ostia, or reducing their length, reduces the flow resistance of the ostia, which will increase the flow through the sinus for a given pressure difference. The models with two ostia of different diameters (*models L* and *M*), with identical ventilation rates, regardless of which ostium was upstream, show that the total flow resistance of the two ostia is more important than their individual characteristics.

The flow within the sinus itself is complex, with a small recirculating region between the ostia. The tapering shape of the sinus deflects the inflow from the ostium from impacting directly on the lateral wall of the sinus, except for the largest ostia. There is a very small recirculation region in the upstream half of the upstream ostium. This recirculation reduces the cross-sectional area available for flow through the ostium and increases the velocity of the flow entering the sinus. If large recirculating regions form in the sinus that do not interact with the flow through the ostia, the overall air replacement rate will be reduced. Otherwise, the shape of the sinus would have a negligible effect on the flow magnitude.

Mucociliary Effects

The modeling of mucociliary velocities on the walls of the sinus, ostium, and middle meatus had no effect on the convective or diffusive exchange time. Gas exchange between the sinus and the nose could be prevented by the formation of a mucous plug in the ostium, but this phenomenon was not modeled during this study. Mucociliary transport is, however, very important to sinus health, as it is the primary mechanism for removal of any pathogens that enter the sinus.

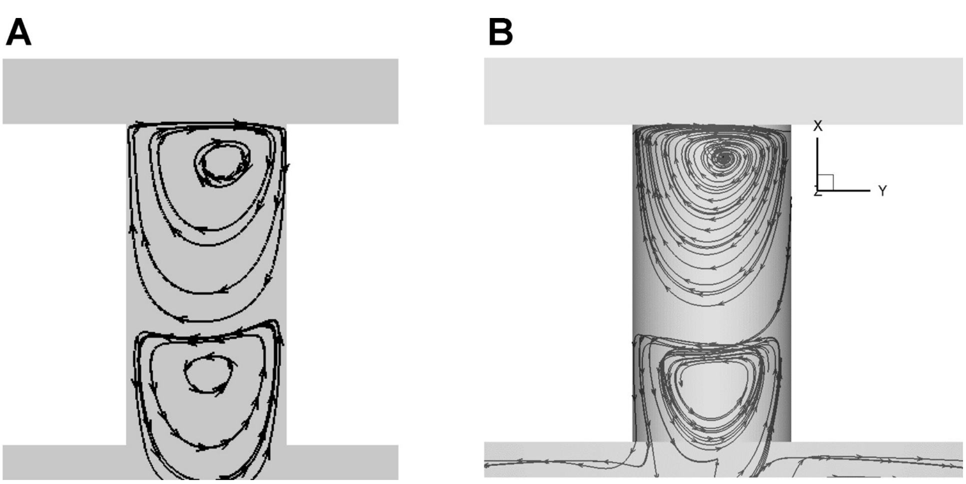

Fig. 8. *A*: 2-dimensional ostium streamlines. *B*: 3-dimensional streamlines.

Diffusion Effects

Diffusion is also responsible for increases in sinus ventilation rates; comparison of 1-D with 3-D computational model results for diffusion with physical model results of Aust and Drettner (3) is given in Table 3. It should be noted that the concentration differences driving diffusion in these models and experiments are much larger than are likely to be the case in normal life, so the natural air replacement times would be longer.

The CFD simulation results for diffusion alone closely match 1-D estimates from Fick's law. The simulation results for diffusion and convection match the results of Aust and Drettner (3) better for larger ostium diameters. The differences may be due to additional ventilation of the sinuses by air leaked through the measurement cannulas. Some difference may be attributable to bidirectional periodic airflow through the nose during the experiments, whereas the simulation has unidirectional steady flow in the middle meatus. Bidirectional flow is likely to cause some additional mixing in the ostium and sinus, as all the vortices change orientation with the direction of nasal airflow. However, the very low air speeds in the vortices and the short time over which they change direction compared with the whole nasal cycle are likely to limit the significance of this mixing.

The order-of-magnitude estimates of NO transport, based on a range of nasal and sinus NO concentrations and production rates previously reported in the literature, do not seem to support the theory that the sinuses produce all or most of the NO detected in air exhaled from the nose. This conclusion is due to the measured rates of NO production by the sinuses being considerably smaller than the measured nasal NO exhalation rates. However, it does seem plausible that the sinus can maintain a high internal NO concentration and supply some of the nasal NO, with measured production rates exceeding the estimated diffusive and convective transport rates through the ostium. NO production rates per unit area of nasal and/or sinus mucosa have not been reported in the literature and are difficult to predict because of the different types and concentrations of NOS found in each tissue. However, it seems unlikely that the sinus mucosal cells can produce NO up to four orders of magnitude faster than nasal mucosal cells, as would be required for nasal NO to originate exclusively in the sinuses.

Humming

The experimental studies by others of humming and nasal NO output have not hypothesized any physical mechanisms that could cause their observations. In the single known attempt at numerical simulation of the process, Menzel et al. (24) used an electrical analogy, including a loudspeaker and a microphone, to replicate their experimental sinus model. The long wavelength of vocal-frequency sound waves compared with the scales of nasal geometry and the resemblance of sinus geometry to that of a Helmholtz resonator suggested that a 1-D acoustic model could be a useful tool for preliminary investigations. Such a model was used during this study, with the sinus described as a nonlinear resonator attached to a duct, based on work by Zhao and Morgans (39). There is considerable uncertainty about the input parameters, such as the magnitude of the pressure wave generated in the nasopharynx by humming and the possibility of small variations in the volume of the sinus due to flexibility of the fontanelle membranes. These uncertainties limit the use of the model to noting that typical sinus geometry has an acoustic resonance in the vocal frequency range without enabling the resulting increase in transport to be quantified. It would be valuable in the future to model the interaction between diffusive and acoustic effects by direct 3-D simulation, but this is prohibitively computationally expensive because of the wide range of temporal and spatial scales involved (5).

Conclusions

Natural single-ostium sinus ventilation is very limited unless the ostium is very large.

Accessory ostia can increase sinus ventilation by around four orders of magnitude, which may be harmful.

Mucociliary transport is important for sinus health but does not increase ventilation.

Diffusion is largely responsible for experimental washout times, as found by Aust and Drettner (3), but probably less important in vivo without artificially high concentration differences. Diffusion is more important for transport through small ostia than large ostia.

It is unlikely that all nasal NO originates in the sinuses due to transport and production limitations.

Further study of the effects of humming and other acoustic phenomena on sinus transport processes is needed, but such phenomena are not well suited to direct computational modeling.

APPENDIX

Solution convergence with mesh density. Three meshes of different densities were created for the standard *model B* geometry to test the mesh independence of the solutions obtained. In Fig. A1, the *x*-velocities along two lines parallel to the ostium axis but off-center are plotted against the *x*-position. $x = 0$ corresponds to the ostium-middle meatus interface, whereas $x = -0.006$ is the ostium-sinus interface. The velocities match very well for the 3×10^6 and 6×10^6 cell meshes, with only a small region of significant difference for the 2.7×10^6 cell mesh. The 3×10^6 cell mesh was used for convection-

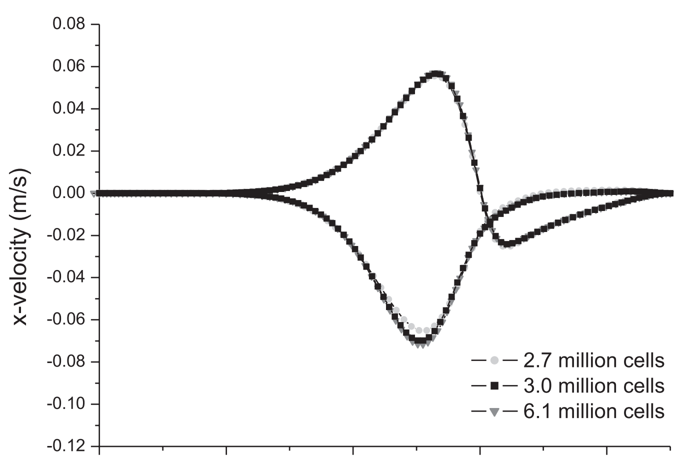

Fig. A1. *x*-Velocities along lines parallel to, but offset from, ostium axis for different mesh densities.

only simulations, and the 6 $\times$ 10^6 cell mesh was used for diffusion simulations.

ACKNOWLEDGMENTS

We thank A. Morgans for help with acoustic modeling and D. Taylor for assistance with Fluent and Gambit.

GRANTS

C. M. Hood is supported by a doctoral training grant from the Biotechnology and Biological Sciences Research Council. R. C. Schroter and D. J. Doorly are supported by a grant from the Biotechnology and Biological Sciences Research Council.

REFERENCES

1. **Andersson JA, Cervin A, Lindberg S, Uddman R, Cardell LA.** The paranasal sinuses as reservoirs for nitric oxide. *Acta Otolaryngol (Stockh)* 122: 861–865, 2002.
2. **Aust R.** Oxygen exchange through the maxillary ostium in man. *Rhinology* 12: 25–37, 1974.
3. **Aust R, Drettner B.** Experimental studies of gas exchange through ostium of maxillary sinus. *Uppsala J Med Sci* 79: 177–186, 1974.
4. **Christie JH, Robinson RG, Kirchner FR, Wegst AV, Herrin WF, Preston DF.** Ventilation and clearance of the sinuses and middle ears using xenon-133. *J Nuclear Med Technol* 8: 23–27, 1979.
5. **Colonius T, Lele SK.** Computational aeroacoustics: progress on nonlinear problems of sound generation. *Prog Aerospace Sci* 40: 345–416, 2004.
6. **Coulson JM, Richardson JF.** *Chemical Engineering*. Oxford, UK: Pergamon, 1971.
7. **Doorly DJ, Taylor DJ, Gambaruto AM, Schroter RC, Tolley N.** Nasal architecture: form and flow. *Philos Trans R Soc A* 366: 3225–3246, 2008.
8. **Drettner B.** The permeability of the maxillary ostium. *Acta Otolaryngol (Stockh)* 60: 304–314, 1965.
9. **DuBois AB, Douglas JS, Stitt JT, Mohsenin V.** Production and absorption of nitric oxide gas in the nose. *J Appl Physiol* 84: 1217–1224, 1998.
10. **Goetzel RZ, Hawkins K, Ozminkowski RJ, Wang S.** The health and productivity cost burden of the "top 10" physical and mental health conditions affecting six large US employers in 1999. *J Occup Environ Med* 45: 5–14, 2003.
11. **Granqvist S, Sundberg J, Lundberg JO, Weitzberg E.** Paranasal sinus ventilation by humming. *J Acoust Soc Am* 119: 2611–2617, 2006.
12. **Guillerm R, Badre R, Flottes L, Riu R, Rey A.** Nouveau procédé assurant la pénétration des aérosols dans les sinus. *La Presse Med* 67: 1097–1098, 1959.
13. **Hess A, Bloch W, Rocker J, Peters S, Stennert E, Addicks K, Michel O.** Nachweis von Stickstoffmonoxidsynthasen bei physiologischen und patho-physiologisch Prozessen in der Nasenschleimhaut. *HNO* 48: 489–495, 2000.
14. **Higdon JJ.** Stokes flow in arbitrary two-dimensional domains—shear flow over ridges and cavities. *J Fluid Mech* 159: 195–226, 1985.
15. **Jog M, McGarry GW.** How frequent are accessory sinus ostia? *J Laryngol Otol* 117: 270–272, 2003.
16. **Kalender WA, Rettinger G, Suess C.** Measurement of paranasal sinus ventilation by xenon-enhanced dynamic CT. *J Comput Assist Tomogr* 9: 524–529, 1985.
17. **Kaliner M, Osguthorpe JD, Fireman P, Anon J, Georgitis J, Davis ML, Naclerio R, Kennedy D.** Sinusitis: bench to bedside. Current findings, future directions. *J Allergy Clin Immunol* 99: S829–S848, 1997.
18. **Lang J.** *Clinical Anatomy of the Nose, Nasal Cavity and Paranasal Sinuses.* Stuttgart: Georg Thieme Verlag, 1989.
19. **Lundberg JON, Farkasszallasi T, Weitzberg E, Rinder J, Lidholm J, Anggard A, Hokfelt T, Lundberg JM, Alving K.** High nitric oxide production in human paranasal sinuses. *Nat Med* 1: 370–373, 1995.
20. **Maniscalco M, Sofia M, Weitzberg E, Lundberg JO.** Sounding airflow enhances aerosol delivery into the paranasal sinuses. *Eur J Clin Invest* 36: 509–513, 2006.
21. **Maniscalco M, Weitzberg E, Sundberg J, Sofia M, Lundberg JO.** Assessment of nasal and sinus nitric oxide output using single-breath humming exhalations. *Eur Respir J* 22: 323–329, 2003.
22. **Marcucci C, Leopold D, Cullen MM, Zinreich SJ, Simon BA.** Dynamic assessment of paranasal sinus ventilation using xenon-enhanced computed tomography. *Ann Otol Rhinol Laryngol* 110: 968–975, 2001.
23. **Matthews BL, Burke AJC.** Recirculation of mucus via accessory ostia causing chronic maxillary sinus disease. *Otolaryngol Head Neck Surg* 117: 422–423, 1997.
24. **Menzel L, Hess A, Bloch W, Michel O, Schuster KD, Gabler R, Urban W.** Temporal nitric oxide dynamics in the paranasal sinuses during humming. *J Appl Physiol* 98: 2064–2071, 2005.
25. **Myerson MC.** The natural orifice of the maxillary sinus. I. Anatomic studies. *Arch Otolaryngol* 15: 80–91, 1932.
26. **Myerson MC.** The natural orifice of the maxillary sinus. II. Clinical studies. *Arch Otolaryngol* 15: 716–733, 1932.
27. **Proctor DF, Andersen I.** *The Nose: Upper Airway Physiology and the Atmospheric Environment*. Amsterdam: Elsevier Biomedical, 1982.
28. **Proetz AW.** *Essays on the Applied Physiology of the Nose*. St. Louis, MO: Annals, 1953.
29. **Proetz AW.** Some intimate studies of nasal function: their bearing on diagnosis and treatment. *Ann Otol Rhinol Laryngol* 41: 125, 1932.
30. **Rantanen T.** Clinical function tests of the maxillary sinus ostium. *Acta Otolaryngol Suppl (Stockh)* 328: 1–38, 1974.
31. **Riu R, Le Den, Pescio.** Traitement des sinusites par les aérosols soniques. *Rev Laryngol* 81: 856–907, 1960.
32. **Scott-Brown WG.** *Scott-Brown's Otolaryngology*. London: Butterworths, 1987.
33. **Shankar PN, Deshpande MD.** Fluid mechanics in the driven cavity. *Annu Rev Fluid Mech* 32: 93–136, 2000.
34. **Simon E.** Anatomy of the opening of the maxillary sinus. *Arch Otolaryngol* 29: 640–649, 1939.
35. **Törnberg DCF, Marteus H, Schedin U, Alving K, Lundberg JO, Weitzberg E.** Nasal and oral contributions to inhaled and exhaled nitric oxide: a study in tracheotomized patients. *Eur Respir J* 19: 859–864, 2002.
36. **Tutty OR.** Flow in a tube with a small side branch. *J Fluid Mech* 191: 79–109, 1988.
37. **van Alyea OE.** The ostium maxillare: anatomic study of its surgical accessibility. *Arch Otolaryngol* 24: 555–569, 1936.
38. **Weitzberg E, Lundberg JON.** Humming greatly increases nasal nitric oxide. *Am J Respir Crit Care Med* 166: 144–145, 2002.
39. **Zhao D, Morgans A.** *Tuned Passive Control of Combustion Instabilities Using Multiple Helmholtz Resonators*. Reston, VA: Am. Inst. Aeronautics Astronautics, 2007, p. 2007–3423.
40. **Zippel R, Streckenbach B.** Xenon washout in the paranasal sinuses: a diagnostic tool for assessing ostial function. *Rhinology* 17 *Suppl*: 25–29, 1979.